Weierstraß-Institut

für Angewandte Analysis und Stochastik

Leibniz-Institut im Forschungsverbund Berlin e. V.

Preprint ISSN 2198-5855

Timing jitter in passively mode-locked semiconductor lasers

Alexander Pimenov[1], Dmitrii Rachinskii[2], Tatiana Habruseva[3,4,5],

Stephen P. Hegarty[3,5], Guillaume Huyet[3,5,6], Andrei G. Vladimirov[1]

submitted: August 18, 2014

[1] Weierstrass Institute
Mohrenstr. 39, 10117 Berlin, Germany
E-Mail: alexander.pimenov@wias-berlin.de
andrei.vladimirov@wias-berlin.de

[2] Department of Mathematical Sciences
The University of Texas at Dallas
800 W. Campbell Road
Richardson, Texas, USA

[3] Tyndall National Institute
University College Cork
Lee Maltings, Dyke Parade, Cork, Ireland

[4] Aston University
Aston Triangle
B4 7ET Birmingham, UK

[5] Centre for Advanced Photonics and Process Analysis
Cork Institute of Technology, Cork, Ireland

[6] National Research University of ITMO
St Petersburg, Russia

No. 1996

Berlin 2014

2010 *Mathematics Subject Classification.* 37N20, 65P30, 78A60.

2010 *Physics and Astronomy Classification Scheme.* 05.45.-a, 42.55.Px, 42.60.Fc, 42.60.Mi, 42.65.Pc.

Key words and phrases. Timing jitter, numerical bifurcation analysis, semiconductor lasers, bistability.

A. P. and A. G. V. acknowledge the support of SFB 787 of the DFG, project B5. T. H. acknowledges support of EU FP7 HARMOFIRE project, Grant No 299288. G. H., S. P. H. and A. G. V. acknowledge the support of EU FP7 PROPHET project, Grant No. 264687. A. G. V. and G. H. acknowledge the support of E. T. S. Walton Visitors Award of the SFI. G. H. and S. P. H. were also supported by the SFI under Contract No. 11/PI/1152, and under the framework of the INSPIRE Structured PhD Programme.

Edited by
Weierstraß-Institut für Angewandte Analysis und Stochastik (WIAS)
Leibniz-Institut im Forschungsverbund Berlin e. V.
Mohrenstraße 39
10117 Berlin
Germany

Fax: +49 30 20372-303
E-Mail: preprint@wias-berlin.de
World Wide Web: http://www.wias-berlin.de/

Abstract

We study the effect of noise on the dynamics of passively mode-locked semiconductor lasers both experimentally and theoretically. A method combining analytical and numerical approaches for estimation of pulse timing jitter is proposed. We investigate how the presence of dynamical features such as wavelength bistability affects timing jitter.

1 Introduction

Semiconductor mode-locked lasers received much attention in the last decade due to their multiple potential applications including high speed optical telecommunications and clocking [2, 3]. Pulses generated by these lasers are affected by noise due to spontaneous emission and other factors such as cavity optical length fluctuations. In particular, their temporal positions in a pulse train deviate from those of the perfectly periodic output. This phenomenon called timing jitter limits the performance of mode-locked devices [9]. Passive mode-locking is an attractive technique for periodic short pulse generation due to simplicity of implementation and handling as compared to other techniques such as hybrid or active mode-locking. However, in the absence of external reference clock passively mode-locked lasers exhibit relatively large pulse timing jitter [11]. Bistable semiconductor lasers can be used as a basic element for optical switches [15, 17] where the timing jitter can play a significant role as well.

Analytical approach to the study of the influence of noise on mode-locked pulses propagating in the laser cavity was developed by H. Haus and A. Mecozzi [7]. Later this technique was extended to include the effects of carrier density in semiconductor lasers [8]. However, many simplifications involved in the analysis of Refs. [7, 8] limit its applicability to modelling dynamics of semiconductor lasers under the influence of noise. In the last two decades extensive numerical simulations of travelling wave [12, 22] and delay differential [13] models were performed to study timing jitter for different laser device configurations. In particular, a monotonous decrease of pulse timing jitter with the increase of injection current in a passively mode-locked semiconductor laser was demonstrated both numerically and experimentally [22]. In this paper using a delay differential equation (DDE) model of a two-section passively mode-locked semiconductor laser [18–20] we study the effect of noise on the characteristics of fundamental mode-locked regime and develop a semianalytical method for estimation of pulse timing jitter, which helps us to avoid high computational cost of a purely numerical approach. With the help of DDE-BIFTOOL [4] we perform numerical bifurcation analysis of the model and demonstrate the existence of bistability between two fundamental mode-locked regimes with different pulse repetition frequencies. By varying the injection current applied to the gain section we demonstrate both experimentally and theoretically three types of the injection current/timing jitter dependence: monotonous decrease of the pulse timing jitter with the increasing injection

current, peaks of timing jitter at certain intermediate values of injection current corresponding to bifurcation points, and abrupt drop of the timing jitter level after a transition between two stable branches of fundamental mode-locked regime occurs. We find both theoretically and experimentally, in some laser samples, timing jitter can be reduced significantly with the additional increase of the injection current, which also shifts the operation frequency.

2 Method

2.1 Delay differential model

We consider a delay differential equation (DDE) model of a two-section passively mode-locked semiconductor laser introduced in [18–20]:

$$\partial_t A + \gamma A = \gamma\sqrt{\kappa}\exp\left\{\frac{1-i\alpha_g}{2}G\left(t-\tau\right) - \frac{1-i\alpha_q}{2}Q\left(t-\tau\right)\right\}A\left(t-\tau\right) + \xi\eta(t), \tag{1}$$

$$\partial_t G = g_0 - \gamma_g G - \left(e^G - 1\right)|A|^2, \tag{2}$$

$$\partial_t Q = q_0 - \gamma_q Q - s\left(1 - e^{-Q}\right)e^G|A|^2, \tag{3}$$

where $A(t)$ is the electric field envelope, $G(t)$ and $Q(t)$ are saturable gain and loss introduced by the gain and absorber sections correspondingly, τ is the cold cavity round-trip time, g_0 and q_0 are unsaturated gain (pump) and absorption parameters, $\alpha_{g,q}$ are linewidth enhancement factors in the gain and absorber sections, $\gamma_{g,q}$ are carrier relaxation rates, γ is the spectral filtering bandwidth, s is a saturation parameter, κ is the linear attenuation factor per cavity round trip, and $\eta(t)$ is δ-correlated Langevin noise of amplitude ξ [13]:

$$\eta(t) = \eta_1(t) + i\eta_2(t),\ \langle\eta_i(t)\rangle = 0,\ \langle\eta_i(t)\eta_j(t')\rangle = \delta_{i,j}\delta(t-t').$$

We denote by $\psi(t) = (\mathrm{Re}\,A, \mathrm{Im}\,A, G, Q)^T$ a real-valued solution of (1).

2.2 Estimation of timing jitter

Due to time shift invariance of the autonomous system of equations (1)-(3) the timing phase of the solution $\psi(t)$ exhibits a random walk under the influence of the white noise [12, 13]. This leads to the appearance of the pulse timing jitter. Hence, in order to estimate timing jitter one needs to separate the phase noise from the amplitude noise. In numerical simulations pulse timing jitter can be estimated directly by calculating the variance of the temporal pulse positions σ_{var} selected in a specific manner from the time series of the electric field $A(t)$ [8,12]. Experimentally, the timing jitter is usually estimated using the root mean square (RMS), σ_{RMS}, of the power spectrum of the pulse train [12, 13, 22]. Estimation of the variance of temporal pulse positions σ_{var} can be done experimentally as well using a second-harmonic non-collinear optical cross-correlation technique, where the relation $\sigma_{RMS} \approx 2.3548\sqrt{2}\sigma_{var}$ holds [8].

In this work we develop a semianalytical method for estimation of pulse timing jitter σ_{var} in DDE model (1)-(3) using a perturbation technique similar to the method proposed by H. Haus and A. Mecozzi [7]. We consider a locally stable fundamental mode-locked solution $\psi_0(t) = (\mathrm{Re}\, A_0, \mathrm{Im}\, A_0, G_0, Q_0)^T$ of system (1)-(3) with $\xi = 0$ (see Fig. 1(a)). This solution satisfies the conditions $|A_0(t)|^2 = |A_0(t - T_0)|^2$, $G_0(t) = G_0(t - T_0)$, and $Q_0(t) = Q_0(t - T_0)$, where the mode-locked pulse period T_0 is close to the cavity round trip time T. Now let us suppose that $\xi \ll 1$. The local dynamics of trajectories of equations (1)-(3) near the periodic solution can be studied using linearisation of the system. Substituting $\psi(t) = \psi_0(t) + \delta\psi(t)$ into (1)-(3) and assuming that $|\delta\psi| \ll 1$ we obtain the following linearized equation:

$$-\frac{d}{dt}\delta\psi(t) + B(t)\delta\psi(t) + C(t-\tau)\delta\psi(t-\tau) + w(t) = 0, \tag{4}$$

where B and C are the Jacobi matrices of the linearisation [1], $w(t) = (\xi\,\mathrm{Re}\,\eta(t), \xi\,\mathrm{Im}\,\eta(t), 0, 0)^T$. The homogeneous system (4) with $w(t) \equiv 0$ has two linearly independent periodic solutions, the so-called neutral modes $\delta\psi_{0\theta} = d\psi_0(t)/dt$ and $\delta\psi_{0\varphi} = (-\mathrm{Im}\, A_0, \mathrm{Re}\, A_0, 0, 0)^T$, which correspond to the time shift and phase shift symmetry of the system (1)-(3), respectively. Next, we project the increment $\psi(T_0) - \psi(0) = \delta\psi(T_0) - \delta\psi(0)$ of the perturbed solution $\psi(t)$ over the period on the neutral eigenfunction $\delta\psi_{0\theta}$ [7] using the variation of parameters formula for DDEs [6].

Let $\delta\psi$ be a solution of homogeneous problem (4) with $w(t) \equiv 0$ and a row vector $\delta\psi^\dagger(t) = (\delta\psi_1^\dagger, \delta\psi_2^\dagger, \delta\psi_3^\dagger, \delta\psi_4^\dagger)$ be a solution of the adjoint problem

$$\frac{d}{dt}\delta\psi^\dagger(t) + \delta\psi^\dagger(t)B(t) + \delta\psi^\dagger(t+\tau)C(t) = 0. \tag{5}$$

For solutions ϕ of (4) and $\phi^\dagger$ of (5) we consider the following bilinear form [5, 6]

$$[\phi^\dagger, \phi](t) = \phi^\dagger(t)\phi(t) + \int_{-\tau}^{0} \phi^\dagger(t+\theta+\tau)C(t+\theta)\phi(t+\theta)d\theta. \tag{6}$$

Adjoint periodic eigenfunctions $\delta\psi_{0\theta}^\dagger$ and $\delta\psi_{0\varphi}^\dagger$ (neutral modes of (5)) are T_0-periodic and satisfy biorthogonality conditions

$$\left[\delta\psi_{0j}^\dagger, \delta\psi_{0k}\right] = \delta_{jk}, \tag{7}$$

where $j, k = \{\theta, \varphi\}$.

Timing jitter σ_{var} is given by the variance of the pulse repetition period fluctuations of the solution $\delta\psi(t)$ projected on the neutral eigenfunction $\delta\psi_{0\theta}$ corresponding to the time shift invariance of the model equations. Using variation of constants formula [6] we obtain

$$\sigma_{var}^2 = \mathsf{var}\left(\int_0^{T_0} \delta\psi_{0\theta}^\dagger(s)w(s)ds\right).$$

For the Langevin term $w(t)$, this expression results in the stochastic Ito integral

$$\sigma_{var}^2 = \xi^2 \mathsf{var}\Bigg(\int_0^{T_0} \delta\psi_{0\theta,1}^\dagger(s)dW_1(s) + \int_0^{T_0} \delta\psi_{0\theta,2}^\dagger(s)dW_2(s)\Bigg),$$

where W_1 and W_2 are two independent Wiener processes. Since the expected value of this integrals is 0, finally, we obtain

$$\sigma_{var}^2 = \xi^2 \int_0^{T_0} \left(\left(\delta\psi_{0\theta,1}^{\dagger}(s) \right)^2 + \left(\delta\psi_{0\theta,2}^{\dagger}(s) \right)^2 \right) ds. \tag{8}$$

Fig. 1(b) indicates that the timing jitter values estimated with the help of asymptotic formula (8) are in good agreement with those obtained numerically from the field amplitude time traces [12, 13].

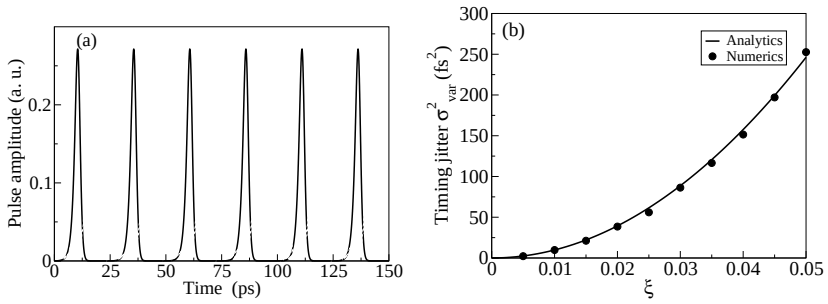

Figure 1: (a) Time traces of the mode-locked solution of Eqs. (1)-(3) at $\xi = 0$ (solid) and $\xi = 0.05$ (dashed). (b) Comparison of results obtained using the asymptotic formula (8) (line) and those of numerical pulse timing jitter calculation from the amplitude time traces (circles) for different values of noise strength ξ. Other parameters are $\tau = 25$ ps, $\kappa = 0.3$, $\gamma^{-1} = 125$ fs, $\gamma_g^{-1} = 500$ ps, $\gamma_q^{-1} = 5$ ps, $q_0^{-1} = 10$ ps, $g_0^{-1} = 250$ ps, $\alpha_q = 1$, $\alpha_g = 2$, $s = 50$.

3 Experiment

The experiments were performed with two-section monolithic quantum-dot mode-locked devices. The active region consisted of 15 layers of InAs quantum-dots grown on GaAs substrate at Innolume GmbH. The devices were cleaved with no coatings applied to the facets and mounted on a temperature controlled stage. We used a set of lasers with different absorber section lengths in the experiments.

Pulse timing jitter fluctuations were measured via the integration of the normalized power spectral density (PSD), $L_{RF}(f)$, over a certain range [21]:

$$\sigma^i(f_1, f_2) = \frac{T_r}{2\pi} \sqrt{2 \int_{f_1}^{f_2} L_{RF}(f) df}, \tag{9}$$

where σ^i is an integrated timing jitter, f_1 and f_2 are the lower and upper integration limits, and T_r is the pulse train period.

The single sideband PSD was measured from the output radio-frequency (RF) spectrum using an Advantest electronic spectrum analyzer (ESA), a fast photodetector, and an amplifier. The

normalized PSD is given by the expression:

$$L_{RF}(f) = \frac{S_{RF}(f)}{RBW \times S_t}, \tag{10}$$

where S_t is the peak signal power, RBW is the resolution bandwidth of the ESA, and $S_{RF}(f)$ is PSD.

The single sideband PSD was integrated over the range of 20 kHz-80 MHz as shown in Fig. 2(a), from both sides. When the RF spectra fit well with the Lorentzian (Fig. 2(a), red) the PSD can be estimated from the Lorentzian fit and multiplied by two.

For the Lorentzian line shape, the integrated timing jitter can be determined from the RF linewidth, $\Delta\nu_{RF,1}$, of the first harmonic in the RF spectrum and pulse train period T_r [10]:

$$\sigma^i(f_1, f_2) = \frac{T_r\sqrt{\Delta\nu_{RF,1}}}{2\pi^{3/2}}\sqrt{\frac{1}{f_1} - \frac{1}{f_2}}. \tag{11}$$

Fig. 2(b) shows measured timing jitter for the lasers P_1 (red) and P_2 (black) with 17% and 12% absorber sections, respectively, as a function of gain current. For the laser P_1 the jitter demonstrated monotonic decrease with the gain current, while for the laser P_2 the integrated jitter behavior was non-monotonic with values ranging from 11 to 23 ps.

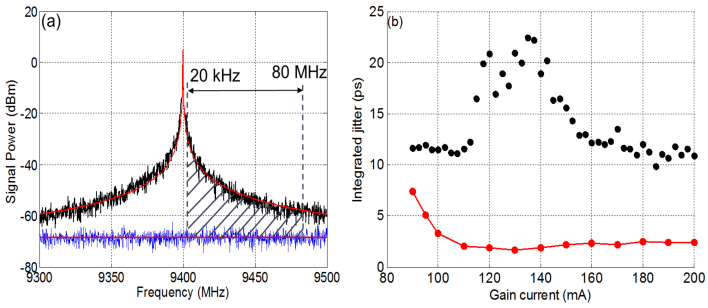

Figure 2: (a) Integration of timing jitter. Measured RF signal (black) and Lorentzian fit (red), laser P_2. (b) Integrated timing jitter for lasers P_1 (red) and P_2 (black) versus gain current.

Fig. 3(a) shows measured RF spectrum evolution versus gain current. The transition between two mode-locked regimes can be seen at the gain current of around 209 mA with a shift of the repetition rate and decrease of jitter. Examples of the RF spectra at the transition point are shown in Fig. 3(b) by black and red lines for the gain currents of 209 mA and 210 mA, respectively. It can be seen that the RF linewidth after the transition point is about twice narrower.

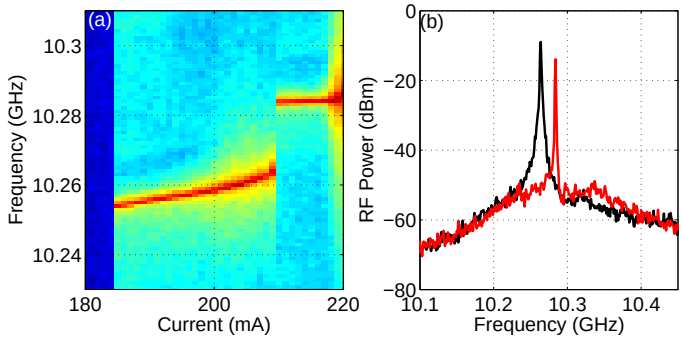

Figure 3: (a) Evolution of the RF spectrum with gain current. (b) RF spectra for the transition point for the gain current of 209 mA (black) and 210 mA (red). Laser P_3, reverse bias -4.0 V.

4 Numerical results

For our numerical analysis we chose the parameters of model equations (1)-(3) to match those of a 10 GHz laser [15] : $\tau = 100ps$, $\gamma^{-1} = 0.5$ ps, $\gamma_g^{-1} = 500$ ps, $\gamma_q^{-1} = 10$ ps, $q_0^{-1} = 5.56$ ps, $\alpha_q = 1$, $\kappa = 0.3$, and the level of noise $\xi = 0.05$ [13].

It has been previously noted that high asymmetry in the phase-amplitude coupling in the gain and absorber sections can be strongly linked to complex dynamical behaviour of semiconductor lasers [20]. This strong coupling can be accounted for by assuming that the difference between linewidth enhancement factors $\alpha_g - \alpha_q$ in the gain and absorber sections is sufficiently large [15]. We chose the pumping parameter g_0 as the continuation parameter to obtain bifurcation diagrams in Fig. 4 with the help of the DDE-BIFTOOL package [4]. The timing jitter was estimated using Eq. (8) by implementing a MATLAB code for calculation of the eigenfunctions of the adjoint eigenproblem (5).

Motivated by the timing jitter comparison performed in the experiment (see Fig. 3) for the bistable branches of fundamental mode-locked regimes with different pulse repetition frequencies, we find that a bistability between two mode-locked regimes exists in the model (1)-(3) for g_0 between 6.058 and 6.06 ns^{-1}, see Fig. 4(a). We see from Fig. 4 (b) that for each of the two branches the timing jitter first decreases with increasing g_0 and then increases towards the instability threshold of the mode-locking regime. Similarly to the experimental results of Fig. 3, timing jitter drops abruptly when the solution switches from the branch staring at the point A to the branch starting at the point B. When the saturation parameter s is increased to 9.5 the fold bifurcations disappear (see dash-dotted line in Fig. 4(a)) and a single branch of mode-locking regime remains stable. However, as it is illustrated by the dash-dotted line in Fig. 4(b) the pulse timing jitter dependence on the pump parameter remains similar to that in the bistable case, demonstrating large peaks near the former instability points. At even higher value of the saturation parameter $s = 11$ the timing jitter dependence still has a smaller peak in the same region. Our simulations performed with the help of the software package DDE-BIFTOOL indicate that these peaks appear when one of the negative Lyapunov exponents of the mode-locked solution $\psi_0(t)$ comes very close to zero with the change of the parameter g_0. Such local increase in the pulse timing jitter obtained numerically for $\alpha_g = 5$ is in agreement with the experimental results

shown in Fig. 2(b) for the laser P_2. Finally, for $s = 24$ we observed monotonous decrease of the pulse timing jitter with the increase of g_0, which is in agreement with the experimental data obtained for the laser P_1.

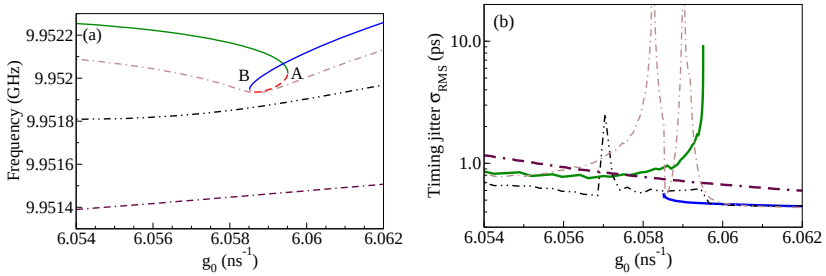

Figure 4: Branches of fundamental ML regime (a) and corresponding timing jitter (b) for $s = 24$ (dash-dash-dotted), $s = 11$ (dash-dot-dotted), $s = 9.5$ (dash-dotted), $s = 8.9$ (solid and dashed for unstable), where A and B are fold bifurcation points. Other parameters are $\gamma^{-1} = 0.5$ ps, $\gamma_g^{-1} = 500$ ps, $\gamma_q^{-1} = 10$ ps, $q_0^{-1} = 5.56$ ps, $\alpha_q = 1$, $\alpha_g = 5$.

5 Conclusion

We have studied theoretically and experimentally the effect of noise on the characteristics of a two-section semiconductor laser operating in fundamental mode-locking regime. We have proposed a semianalytical method for estimation of timing jitter in a system of DDEs (1)-(3) describing this laser. The proposed method can be applied to study noise characteristics of other multimode laser devices modeled by systems of delay-differential equations [13, 14, 16]. Using the software package DDE-BIFTOOL we have studied the dependence of the timing jitter on the injection current and other laser parameters and, in contrast to previous theoretical results [22], we have demonstrated that this dependence can be non-monotonous. Specifically, we have observed a peak in the gain dependence curve of timing jitter, which is related to the presence of a real Lyapunov exponent approaching zero from below. Our results suggest that in the bistable regime of operation the branch of mode-locking regime that is stable at lower injection currents exhibits higher level of pulse timing jitter. A sudden drop in the timing jitter is observed when the laser switches to another branch of mode-locking regime with the increase of the injection current.

References

[1] R. Arkhipov, A. Pimenov, M. Radziunas, D. Rachinskii, A. G. Vladimirov, D. Bimberg, and et al. Hybrid mode-locking in semiconductor lasers: simulations, analysis and experiments. IEEE Jornal of Selected Topics in QE, 99:1100208, 2013.

[2] P. J. Delfyett, S. Gee, M.-T. Choi, H. Izadpanah, W. Lee, S. Ozharar, F. Quinlan, and T. Yilmaz. Optical frequency combs from semiconductor lasers and applications. J. Lightwave Technol, 24:27012719, 2006.

[3] Marcia Costa e Silva, Alexandra Lagrost, Laurent Bramerie, Mathilde Gay, Pascal Besnard, Michel Joindot, Jean-Claude Simon, Alexandre Shen, and Guan-Hua Duan. Up to 427 GHz All Optical Frequency Down-Conversion Clock Recovery Based on Quantum-Dash Fabry-Perot Mode-Locked Laser. J. Lightwave Technol., 29 (4), 2011.

[4] K. Engelborghs, T. Luzyanina, and G. Samaey. DDE-BIFTOOL v.2.00: A MATLAB package for bifurcation analysis of delay differential equations. Technical Report TW-330, Department of Computer Science, K.U.Leuven, Leuven, Belgium, 2001.

[5] A. Halanay. Differential Equations: Stability, Oscillations, Time Lags. Academic Press, 1966.

[6] J. Hale. Theory of Functional Differential Equations. Springer-Verlag, 1977.

[7] H. A. Haus and A. Mecozzi. Noise of mode-locked lasers. IEEE JQE, 29(3):983–995, 1993.

[8] L. Jiang, M. E. Grein, H. A. Haus, and E. P. Ippen. Noise of mode-locked semiconductor lasers. IEEE Jornal of Selected Topics in QE, 7(2):159–167, 2001.

[9] Leaf A. Jiang, Matthew E. Grein, Erich P. Ippen, Cameron McNeilage, Jesse Searls, and Hiroyuki Yokoyama. Quantum-limited noise performance of a mode-locked laser diode. Opt. Lett., 27(1):49–51, Jan 2002.

[10] F. Kéfélian, S. O'Donoghue, M. T. Todaro, J. G. McInerney, and G. Huyet. RF Linewidth in Monolithic Passively Mode-Locked Semiconductor Laser. IEEE Photon. Tech. Lett., 20 (16), 2008.

[11] Chang-Yi Lin, Frederic Grillot, Yan Li, Ravi Raghunathan, and Luke F. Lester. Characterization of timing jitter in a 5 ghz quantum dot passively mode-locked laser. Opt. Express, 18(21):21932–21937, Oct 2010.

[12] J. Mulet and J. Mork. Analysis of timing jitter in external-cavity mode-locked semiconductor lasers. IEEE JQE, 42(3):249–256, 2006.

[13] C. Otto, K. Lüdge, A. G. Vladimirov, M. Wolfrum, and E. Schöll. Delay-induced dynamics and jitter reduction of passively mode-locked semiconductor lasers subject to optical injection. New Journal of Physics, 14:113033, 2012.

[14] A. Pimenov, V. Z. Tronciu, U. Bandelow, and A. G. Vladimirov. Dynamical regimes of a multistripe laser array with external off-axis feedback. J. Opt. Soc. Am. B, 30(6):1606–1613, Jun 2013.

[15] A. Pimenov, E. A. Viktorov, S. P. Hegarty, T. Habruseva, G. Huyet, D. Rachinskii, and A. G. Vladimirov. Bistability and hysteresis in an optically injected two-section semiconductor laser. Phys. Rev. E, 89:052903, May 2014.

[16] N. Rebrova, G. Huyet, D. Rachinskii, and A. G. Vladimirov. Optically injected mode-locked laser. Physical Review E, 83:066202, 2011.

[17] K. Silverman, M. Feng, R. Mirin, , and S. Cundiff. Exotic behavior in quantum dot mode-locked lasers: Dark pulses and bistability. In Quantum Dot Devices, volume 13 of Lecture Notes in Nanoscale Science and Technology, pages 23–48. Springer-Verlag, NY, 2012.

[18] A. G. Vladimirov and D. Turaev. New model for mode-locking in semiconductor lasers. Radiophys. & Quant. Electron., 47(10-11):857–865, 2004.

[19] A. G. Vladimirov and D. Turaev. Model for passive mode-locking in semiconductor lasers. Phys. Rev. A, 72:033808 (13 pages), 2005.

[20] A. G. Vladimirov, D. Turaev, and G. Kozyreff. Delay differential equations for mode-locked semiconductor lasers. Opt. Lett., 29:1221–1223, 2004.

[21] D. von der Linde. Characterization of the Noise in Continuously Operating Mode-Locked Lasers. Appl. Phys. B, 39, 1988.

[22] B. Zhu, I. H. White, R. V. Penty, A. Wonfor, E. Lach, and H. D. Summers. Theoretical analysis of timing jitter in monolithic multisection mode-locked dbr laser diodes. IEEE JQE, 33(7):1216–1220, 1997.